Photoacoustic Imaging Using a 9F MicroLinear CMUT ICE Catheter

Amin Nikoozadeh[1], Jung Woo Choe[1], Sri-Rajasekhar Kothapalli[1], Azadeh Moini[1], Sahinaz S. Sanjani[1], Aya Kamaya[1], Ömer Oralkan[2], Sanjiv S. Gambhir[1], and Pierre T. Khuri-Yakub[1],

1 Stanford University, Stanford, CA, **2** North Carolina State University, Raleigh, NC

Abstract — **This work presents our preliminary results on developing a multi-modality imaging catheter enabling combined ultrasound and photoacoustic imaging. We have developed an optical fiber ring catheter for use with our previously demonstrated 9F, real-time, forward-looking intracardiac ultrasound imaging catheter. Our custom software provides real-time ultrasound and photoacoustic imaging on a PC-based imaging platform. The promising phantom and *in vivo* imaging results presented here demonstrate the utility of a fully integrated catheter that provides both anatomical and functional information through co-registered ultrasound and photoacoustic imaging capabilities.**

Keywords – photoacoustic; ultrasound; catheter; real-time; intracardiac echocardiography; forward-looking; capacitive micromachined ultrasonic transducers; CMUT

e-mail contact: aminn@stanford.edu

I. Introduction

Photoacoustic imaging is a valuable imaging modality that provides functional information about the biological tissue of interest; it is even more useful when complemented by ultrasound imaging for anatomical information. Integrating an ultrasound imaging catheter with optical fibers creates a dual-modality imaging catheter for co-registered anatomical and functional information.

Our previous efforts have been concentrated on multi-functional intracardiac echocardiography (ICE) catheters to improve the electrophysiological (EP) procedures' outcome compared to fluoroscopy alone [1-3]. Addition of photoacoustic imaging capability to these catheters provides even more value through functional information. Such catheters can be utilized in a variety of applications such as cancer, lesion, and plaque detection, and in particular, cases where small size is required for minimally invasive procedures.

In this work, we are investigating the utility of an integrated forward-looking catheter capable of dual-modality, ultrasound and photoacoustic imaging. This paper provides a brief overview of the previously developed 9F (3 mm) ICE catheter, the newly developed optical fiber ring catheter and the software used for combined ultrasound and photoacoustic imaging. Preliminary characterization and imaging results will also be presented.

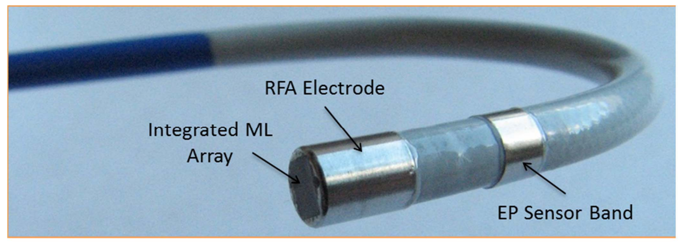

Figure 1. Photograph of 9F ML CMUT catheter tip. This catheter is equipped with an integrated CMUT phased array, an RF ablation (RFA) electrode, and an EP sensor band for 3-D anatomical mapping.

II. Methods

A. CMUT ICE Catheter

We have previously developed a 9F forward-looking ICE catheter for real-time guidance of EP interventions, namely MicroLinear (ML) catheter (Fig.1) [4]. The ML catheter consists of a 24-element, 1-D capacitive micromachined ultrasonic transducer (CMUT) array for phased-array imaging. The transducer die measures 1.7 mm x 1.3 mm and provides an active aperture of approximately 1.5 mm by 1.1 mm in azimuth and elevation directions, respectively. The CMUT arrays were fabricated using the polysilicon sacrificial release process with through-wafer electrical vias [5]. These through-wafer interconnects provide all the required electrical connections to the transducer through pads on the backside of the die, enabling tight integration with supporting electronics.

Each ML array element has a capacitance of approximately 2 pF, which is quite small compared to a coaxial cable capacitance of approximately 200 pF in a typical catheter assembly. Thus, direct connection of these small array elements to an imaging system would yield low SNR and in turn poor image quality. Therefore, we designed a custom front-end IC to be closely integrated with the ML array at the tip of the catheter. The chosen IC architecture enables seamless integration with standard imaging systems since it uses a shared single pad for both transmit and receive paths; therefore, each channel requires a single cable, same as any standard transducer [4]. Each IC channel provides a dedicated low-noise preamplifier for each transducer array element. It also provides an internal path for external high-voltage transmit pulses of up to ±50 V. The IC provides an improvement of approximately 18 dB in noise figure (NF) over direct connection to a typical imaging system (Fig. 2), translating into 18-dB improvement in SNR.

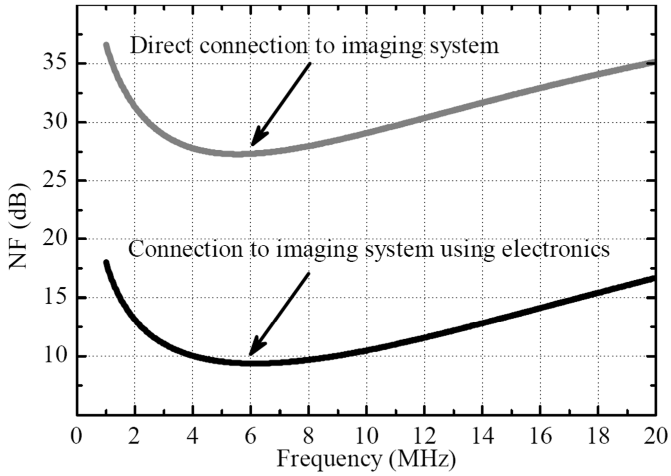

Figure 2. Overall NF simulation results of ML CMUT array element connected to a typical imaging system using a 2-m long, 48-AWG coaxial cable, with and without the custom front-end IC.

The ML CMUT array and the front-end IC were integrated using flip-chip bonding through an intermediate custom flexible PCB. After the integration, the flexible PCB was reshaped for final catheter assembly with the catheter shaft. Coaxial cable termination pads are also provided on the two ends of the flexible PCB.

We have previously demonstrated the full catheter assembly process and packaged several devices, all of which were fully functional. Further, we have demonstrated their *in vivo* imaging performance using porcine animal heart models.

B. Optical Fiber Ring Catheter

An optical fiber ring catheter was designed and manufactured to enable photoacoustic imaging with the ML catheter. The optical catheter contains a multi-mode fiber bundle designed to focus the donut-shaped laser beam 5 mm away from its distal end. The ML catheter is simply inserted into the optical ring catheter and navigated to its distal end for dual-modality imaging (Fig. 3).

Our first generation of the optical catheter is relatively large, having an 8-mm outside diameter, to allow for better investigation of its light delivery capability and assure mechanical rigidity. This catheter has a lumen slightly larger than 3 mm, specifically designed for the 9F ML catheter. As seen in Fig. 3, the optical catheter provides an input to couple the laser light into the catheter and another entrance for the ML CMUT catheter.

C. Real-Time Dual-Modality Imaging

A PC-based imaging platform from Verasonics (Verasonics, Inc., Redmond, WA) is used for data acquisition and synchronization. We developed a custom imaging software that enables combined ultrasound and photoacoustic imaging on this platform.

Figure 4 shows a simplified block diagram of the imaging sequence used for dual-modality imaging. Our photoacoustic data acquisition and image reconstruction rate is currently limited by the repetition rate of our pulsed OPO laser at 10 Hz. Therefore, every 100 ms a single frame of photoacoustic image

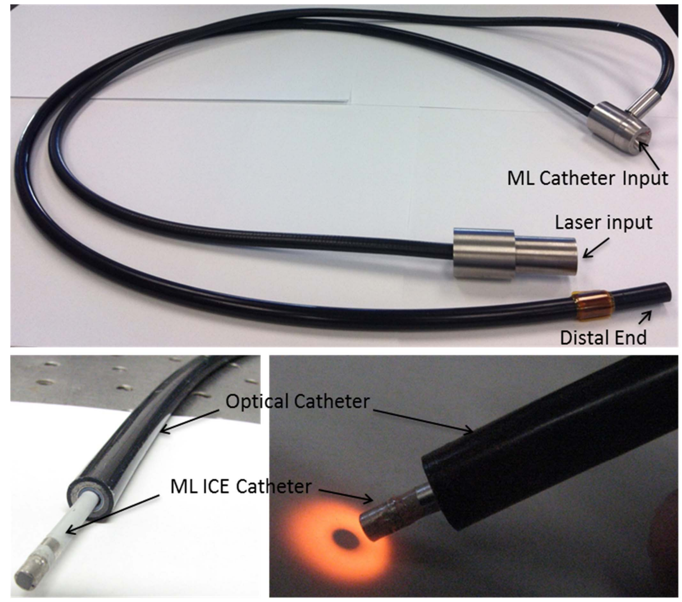

Figure 3. Optical fiber ring catheter. Top photograph shows the whole catheter and the bottom images show the distal end of the catheter with the ML ICE catheter through it.

data is acquired and processed. The Verasonics platform is responsible for the trigger signal and synchronization. After each photoacoustic data acquisition, ultrasound pulse-echo data is acquired for as many frames as possible until the next laser trigger signal. Classic phased-array imaging is used for ultrasound imaging, and receive-only dynamic focusing is used for photoacoustic imaging.

Our imaging interface provides three B-mode display panels, one for each of the ultrasound, photoacoustic, and the overlaid ultrasound and photoacoustic images. Ultrasound image is displayed in grayscale while the photoacoustic image is shown using different shades of red. Among other functionalities, the interface provides independent, real-time control of compression and display dynamic range of the ultrasound and photoacoustic images.

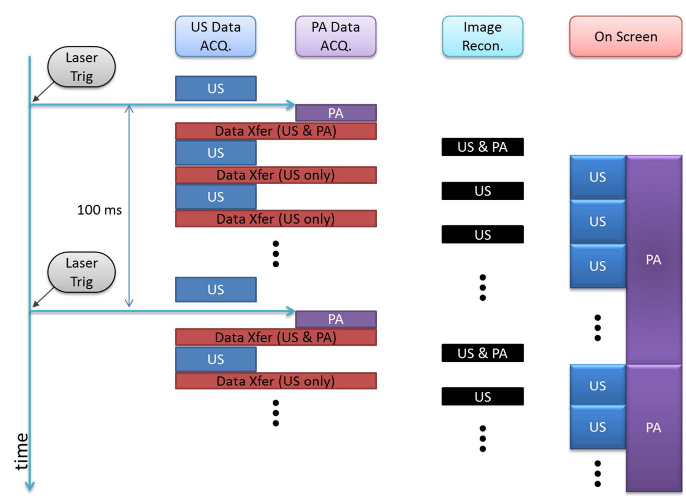

Figure 4. Imaging sequence used for combined ultrasound and photoacoustic imaging using Verasonics platform. Photoacoustic image frames are acquired at a rate of 10 Hz, limited by our laser repetition rate; the rest of the time is filled with as many ultrasound image frames as possible.

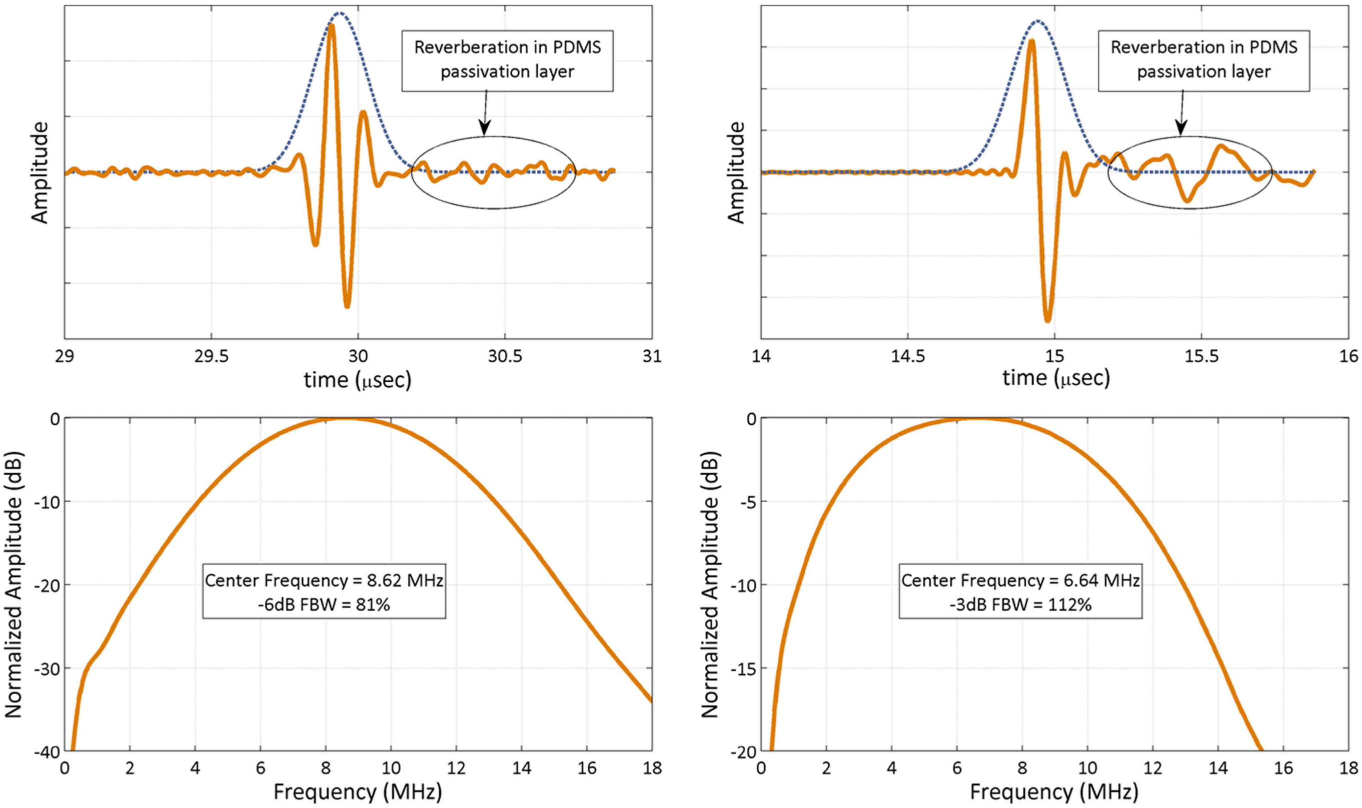

Figure 5. Pulse-echo (left column) and photoacoustic (right column) signals from an aluminum plate in water for a single ML CMUT array element. The transient signals and their corresponding frequency spectrums are shown on top and bottom rows, respectively.

III. Results

A. Characterization

We measured the single-element pulse-echo and photoacoustic signals from an aluminum plate, placed about 22 mm away from the transducer surface in water (Fig. 5). The CMUT array was biased at 60 V for both measurements. The AC excitation for the pulse-echo experiment was a 55 V_{p-p} bipolar pulse.

This particular catheter uses a passivation layer material that is poorly matched to water or tissue, and hence, results in unwanted reverberations that are clear in the transient signals (Fig. 5). We have since moved to another passivation layer material that is significantly better matched to water, and hence, suffers much less from these unwanted reverberations.

B. Imaging Results

We characterized the dual-modality imaging performance of our catheter using imaging phantoms and *in vivo* tumor models. For these experiments, the ML CMUT array was biased at 50 V, and the AC pulse excitation amplitude for ultrasound imaging was 55 V_{p-p}. As previously mentioned, our photoacoustic imaging had a rate of 10 frames per second (fps), limited by the laser repetition rate.

We constructed an intralipid imaging phantom with embedded pencil leads, and dark and clear nylon fishing lines (Fig. 6). The acquired image for this phantom is shown in Fig. 7. The ultrasound image in this experiment was processed at a rate of 40 fps. The photoacoustic image was acquired at a wavelength of 800 nm. It is seen from the reconstructed image that all the targets are visible in the ultrasound image while only the dark-color targets are captured in the photoacoustic image.

We also demonstrated the *in vivo* imaging performance of the integrated catheter using a mouse subcutaneous kidney tumor model (Fig. 8). Due to a shorter imaging depth than the phantom experiment, the ultrasound image in this experiment was processed at a rate of 100 fps. The photoacoustic image was acquired at a wavelength of 740 nm. It is seen from Fig. 8 that the ultrasound image shows the tumor boundary and the

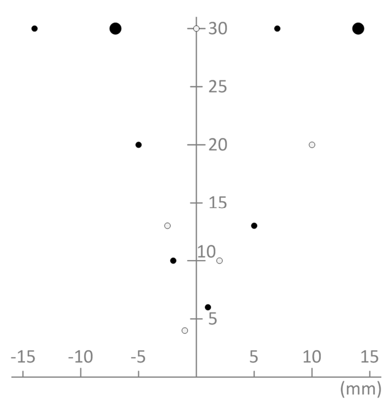

Figure 6. Intralipid imaging phantom with embedded 0.7 mm pencil leads (large black circle), 0.5 mm dark nylon fishing lines (small black circles), and 0.5 mm clear nylon fishing lines (small clear circles). The intralipid medium has an absorption coefficient of 0.1 cm^{-1} and a reduced scattering coefficient of 8 cm^{-1}.

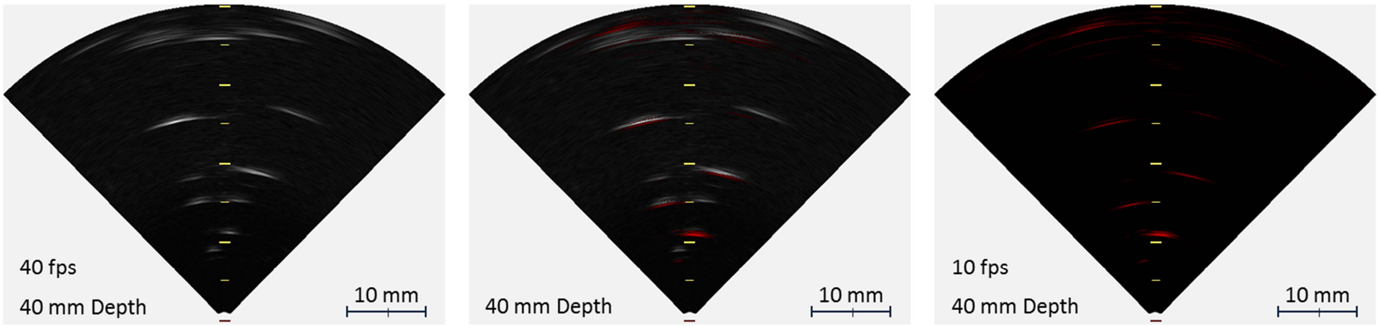

Figure 7. Image of intralipid phantom of Fig. 6. Left, right, and middle panels show the ultrasound, photoacoustic, and the combined images, respectively. Ultrasound image shows all the targets, while the photoacoustic image only shows the dark-color targets.

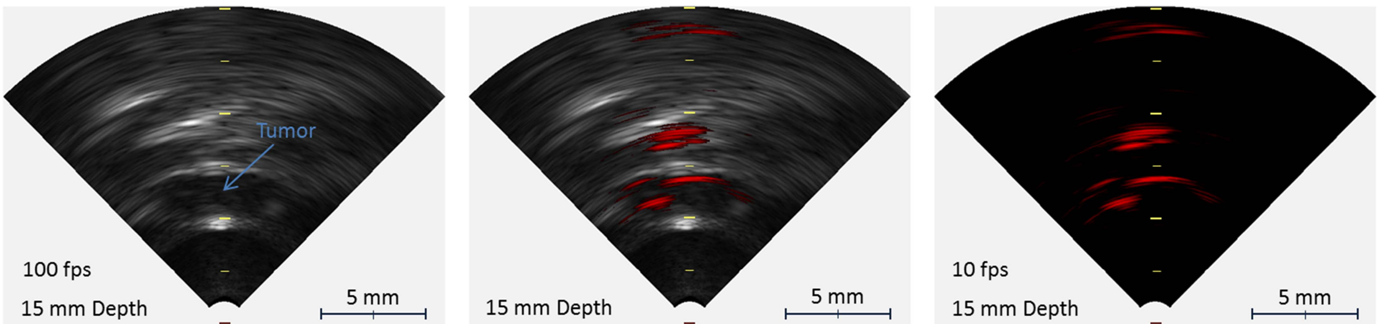

Figure 8. In vivo image of mouse subcutaneous kidney tumor model. Left, right, and middle panels show the ultrasound, photoacoustic, and the combined images, respectively. Tumor boundary and the vasculature within the tumor are visible in the ultrasound and photoacoustic images, respectively.

photoacoustic image provides a view of the vasculatures within the tumor, complementing the ultrasound image.

IV. Conclusion and Future Work

We have successfully demonstrated the utility of our first-generation integrated catheter for combined ultrasound and photoacoustic imaging using preliminary phantom and *in vivo* imaging experiments.

We plan to incorporate multi-wavelength functional imaging capability to our imaging platform (e.g., for oxygen saturation measurement). We will conduct additional *in vivo* animal experiments with contrast agents such as indocyanine green (ICG). In addition to a new smaller optical fiber ring catheter design for our ML catheter, we will design another optical fiber catheter that would allow photoacoustic imaging with our previously developed Ring CMUT catheter for volumetric imaging [6].

Acknowledgment

This work was funded by the National Institutes of Health under grant NHLBI R01-HL67647, USA. We would like to thank Texas Instruments (former National Semiconductor Corporation, Santa Clara, CA) for their valuable support in the design and fabrication of the IC. CMUT fabrication was done at the Stanford Nanofabrication Facility (Stanford, CA), which is a member of National Nanotechnology Infrastructure Network. Solder bumping was provided by Pac Tech USA Inc. (Santa Clara, CA). We would like to thank Charlie Holtan (Precision Interconnects, Wilsonville, OR) for his valuable support on catheter cabling. We also thank Verasonics for their programming support.

References

[1] J. W. Hirshfeld Jr., S. Balter, J. A. Brinker, et al., "ACC F/AHA/HRS /SCA I clinical competence statement on physician knowledge to optimize patient safety and image quality in fluoroscopically guided invasive cardiovascular procedures: A report of the American College of Cardiology Foundation/American Heart Association/American College of Physicians Task Force on Clinical Competence and Training," *J. Am. Coll. Cardiol*., vol. 44, no. 11, pp. 2259–2282, 2004.

[2] M. C. Burke, M. J. D. Roberts, and B. P. Knight, "Integration of cardiac imaging and electrophysiology during catheter ablation procedures for atrial fibrillation," *J. Electrocardiol*., vol. 39, no. 4, pp. S188–S192, 2006.

[3] M. Jongbloed, M. Schalij, K. Zeppenfeld, P. Oemrawsingh, E. van der Wall, J. Bax, "Clinical applications of intracardiac echocardiography in interventional procedures," *Heart*, vol. 91, pp. 981-990, 2005.

[4] A. Nikoozadeh, O. Oralkan, M. Gencel, et al, "Forward-Looking Intracardiac Imaging Catheters Using Fully Integrated CMUT Arrays," in *Proc. IEEE Ultrason. Symp.,* vol. 1, 2010, pp. 770-773.

[5] A. S. Ergun, Y. Huang, X. Zhuang, O. Oralkan, G. G. Yaralioglu, and B. T. Khuri-Yakub, "Capacitive micromachined ultrasonic transducers: Fabrication technology," *IEEE Trans. Ultrason. Ferroelect., Freq. Contr.*, vol. 52, no. 12, pp. 2242–2258, 2005.

[6] A. Nikoozadeh, O. Oralkan, M. Gencel, et al, "Forward-looking volumetric intracardiac imaging using a fully integrated CMUT ring array," in *Proc. IEEE Ultrason. Symp.*, vol. 1, 2009, pp. 511-514.